SUPPORTING INFORMATION

Correlation between the Open Circuit Voltage and the Energetics of Organic Bulk Heterojunction Solar Cells

*Ilja Lange,[1] Juliane Kniepert,[1] Patrick Pingel,[1] Ines Dumsch,[2] Sybille Allard,[2] Silvia Janietz,[3] Ullrich Scherf,[2] and Dieter Neher [1]**

[1] Institute of Physics and Astronomy, University of Potsdam, Karl-Liebknecht-Strasse 24-25, 14476 Potsdam, Germany

[2] Macromolecular Chemistry and Institute for Polymer Technology, Bergische Universität Wuppertal, Gauss-Strasse 20, D-42097 Wuppertal, Germany

[3] Frauenhofer Institut für Angewandte Polymerforschung, Geiselbergstrasse 69, 14476 Potsdam, Germany

A) Full names and chemical structures of the used materials:

$PC_{70}BM$ (Phenyl-C_{71}-butyric-acid-methyl ester)

ICBA (Indene-C60 bisadduct)

P3HT (Poly(3-hexylthiophen-2,5-diyl)

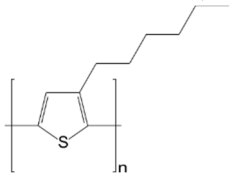

PCPDTBT (Poly[2,6-(4,4-bis(2-ethylhexyl)-4H-cyclopenta[2,1-b;3,4-b′]dithiophene)-alt-4,7-(2,1,3-benzothiadiazole])

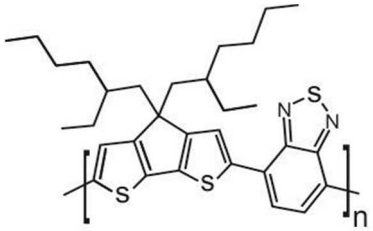

F-PCPDTBT (Poly[2,6-(4,4-bis(2-ethylhexyl)-4H-cyclopenta[2,1-b;3,4-b′]dithiophene)-alt-4,7-(5-fluoro-2,1,3-benzothiadiazole])

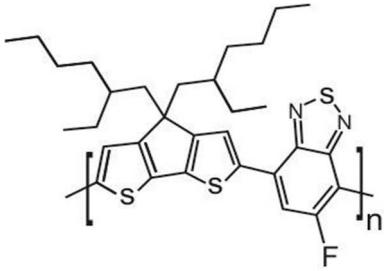

B) Further information on BACE measurements

The main goal of bias amplified charge extraction with respect to conventional charge extraction is to accelerate the extraction of photogenerated charge, thereby preventing recombination and losses due to trapping. Whereas "well-behaving" systems like annealed P3HT:PCBM with a low recombination coefficient and roughly equally high electron and hole mobilities show a negligible dependence of

extracted charge on applied reverse bias, V_{rb}, some novel blends often suffer from high recombination coefficients.

Figure S1a shows the extracted charge as function of applied extraction bias of F-PCPDTBT:PCBM. Above 7 V the curve levels out, from what the extraction of almost all photogenerated carriers can be concluded. It has to be noted that the collected charge under these conditions is about factor 3 higher than without extraction bias. In our measurements we applied a V_{rb} of 5-6 V to the P3HT:PCBM devices and 7-10 V to all other devices.

The respective F-PCPDTBT:PCBM transients for V_{rb} = 0V or 10V are shown in Figure S1b. Fitting the transient decay with an exponential function reveals an extraction time constant τ_{extr} of about 1.5 µs without bias and a 20-fold decrease to about 80 ns when a V_{rb} of 10 V is applied. This accelerated extraction might not completely prevent any recombination, however, at least such effects get strongly depressed enabling also an exact investigation of photogenerated carrier densities in systems with high recombination coefficients.

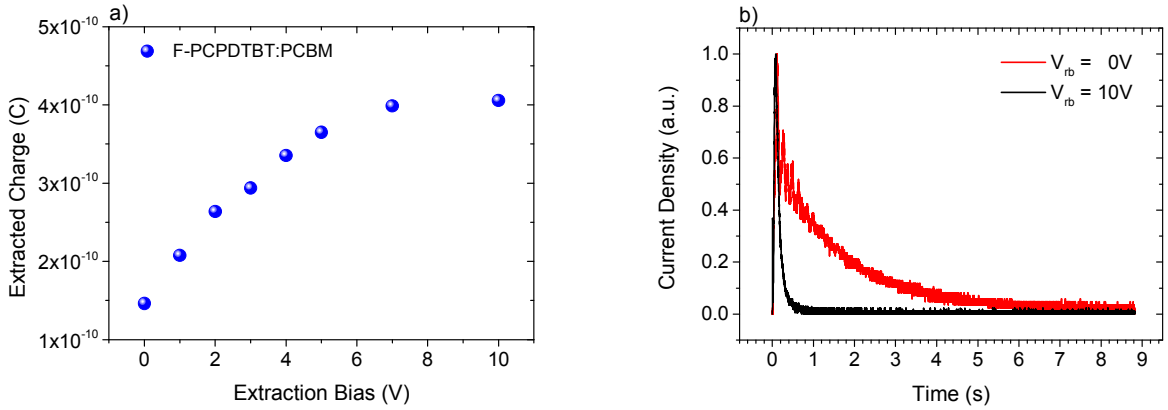

Figure S1: (a) Extracted photogenerated charge as function of reverse extraction bias V_{rb} of F-PCPDTBT:PCBM solar cells. Above 7V the curve levels out pointing to a complete extraction. (b) Respective transients with V_{rb} = 0V and V_{rb} = 10V. Due to the applied bias, the extraction is accelerated by a factor of 20.

Influence of delay between switch-off of the LEDs and application of the reverse extraction bias in BACE experiments

BACE experiments were performed with an either 0 ns and a 220 ns delay between initiation of the LED switch-off and application of the reverse extraction bias. In case of P3HT:PCBM (1:1 annealed), no difference between the extracted carrier density is observed for the two different delay times. Apparently, the amount of additional charge photogenerated during the 200 ns LED switch-off time is very small. In addition, the small bimolecular recombination coefficient in the P3HT:PCBM blend limits the amount of photogenerated charge lost by non-geminate recombination during the delay time. In contrast, for PCPDTBT:PCBM, a longer delay leads to a slightly smaller amount of extracted charge particularly at high carrier densities, which we assign to weak non-geminate recombination during the 220 ns delay.

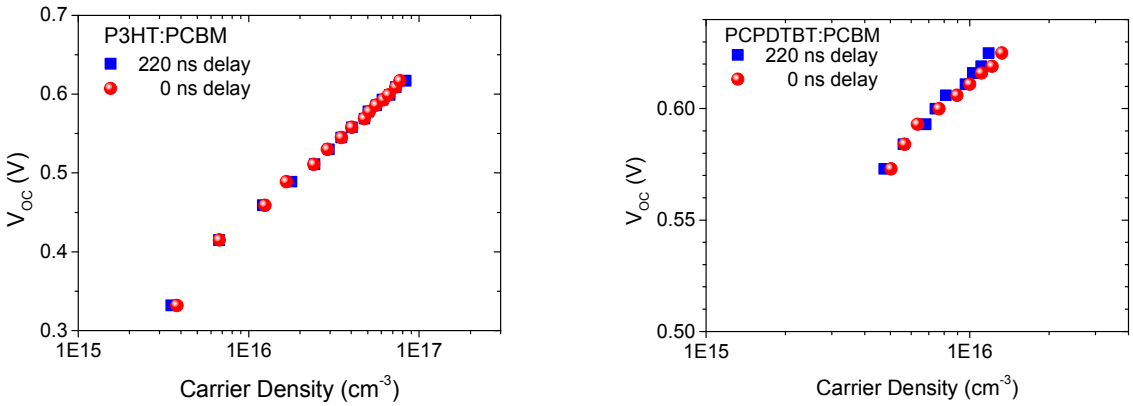

Figure S2: Charge carrier density extracted in BACE with a 0 ns and 220 ns delay for P3HT:PCBM and PCPDTBT:PCBM.

C) Evaluation of $V_{OC}(n)$-relations for different density of states distributions

In Fermi-Dirac statistics, the carrier density is given by

$$n = \int_{-\infty}^{\infty} \frac{1}{e^{\frac{E-E_F}{kT}} + 1} * g(E)dE \,,$$

where the first part of the right hand side is the Fermi-Dirac distribution and *g(E)* is the density of states distribution. To perform the integration analytically, the Fermi-Dirac distribution is replaced by the Boltzmann approximation and the lower boundary is set equal to E_F:

$$n = \int_{E_F}^{\infty} e^{\left(\frac{E_F-E}{kT}\right)} * g(E)dE$$

In case of no disorder, $g(E)$ is set equal to G_0 for $E \geq E_{CB}$, with E_{CB} the onset of the conduction band, and $g(E) = 0$ for $E < E_{CB}$. Thus,

$$n = G_0 \int_{E_{CB}}^{\infty} e^{\left(\frac{E_F-E}{kT}\right)} dE$$

$$= kTG_0 e^{\left(\frac{E_F-E_{CB}}{kT}\right)}.$$

Therefore,

$$E_F - E_{CB} = kT * \ln\left(\frac{n}{kTG_0}\right).$$

Setting $N_0 = kTG_0$ yields:

$$E_F - E_{CB} = kT * \ln\left(\frac{n}{N_0}\right).$$

The expression for the valence band is equivalent. If both types of carriers are present, the splitting of the QFL is given by

$$\Delta E_{F,e,h} = eV_{OC} = (E_{CB} - E_{VB}) + kT\ln\left(\frac{np}{(kT)^2 G_{0,e} G_{0,h}}\right)$$

$$= (E_{CB} - E_{VB}) + kT\ln\left(\frac{np}{N_e N_h}\right)$$

Under the assumption of an exponential DOS $g(E) = G_0 \exp\left(\frac{E-E_{CB}}{E_t}\right)$ (with trap energy E_t and the total site density $N_0 = E_t\, G_0$), the carrier density is determined by:

$$n = \int_{E_F}^{\infty} e^{\left(\frac{E_F - E}{kT}\right)} * G_0\, e^{\left(\frac{E-E_{CB}}{E_t}\right)}\, dE$$

$$= \frac{N_0}{E_t} * \frac{kTE_t}{E_t - kT} e^{\left(\frac{E_F - E_{CB}}{E_t}\right)}$$

Therefore,

$$E_F - E_{CB} = E_t * \ln\left(\frac{n}{N_0} * \left(\frac{E_t}{kT} - 1\right)\right) \approx E_t * \ln\left(\frac{n}{N_0}\right).$$

The second solution is only applicable if $E_t > kT$. With $m = \frac{E_t}{kT}$, this leads to

$$\Delta E_{F,e,h} = eV_{OC} = (E_{CB} - E_{VB}) + mkT * \ln\left(\frac{np}{N_e N_h}\right).$$

D) Display of KP measurements on P3HT:PCBM blends with 2:3 and 3:2 composition

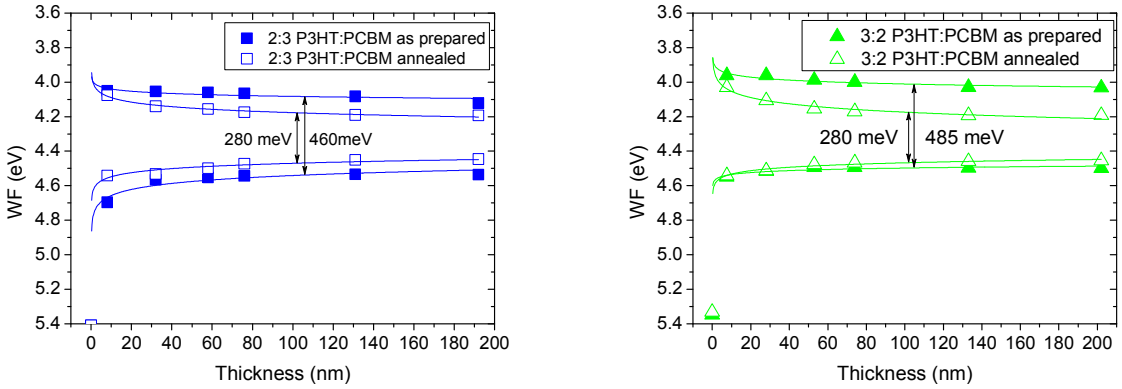

Figure S3: Work function values measured by Kelvin Probe on P3HT:PCBM blends with two different compositions as a function of layer thickness. Blends have been coated either on PEDOT:PSS (lower curves) or Al (upper curves). The differences in the pinning levels of hole and electrons at a thickness of ca. 100 nm are indicated by arrows in both figures and the plotted values have an uncertainty of $\pm$ 25 meV.

E) Thickness-dependent absorption data of 1:1 P3HT:PCBM blends

The normalized absorbance spectra of both as-prepared and annealed P3HT:PCBM (1:1) reveal a continuous increase of the 600 nm peak strength with decreasing layer thickness, which we attribute to a larger degree of crystallinity in the part of the layer close to the substrate. Thus, the morphology and with that the energetics are not constant throughout the blend film. The analysis of the thickness dependent WF data with regard to the density of states distribution in the layer according to Lange *et al.* (*Phys. Rev. Lett.* **2011**, 106, 216402) is, therefore, not possible.

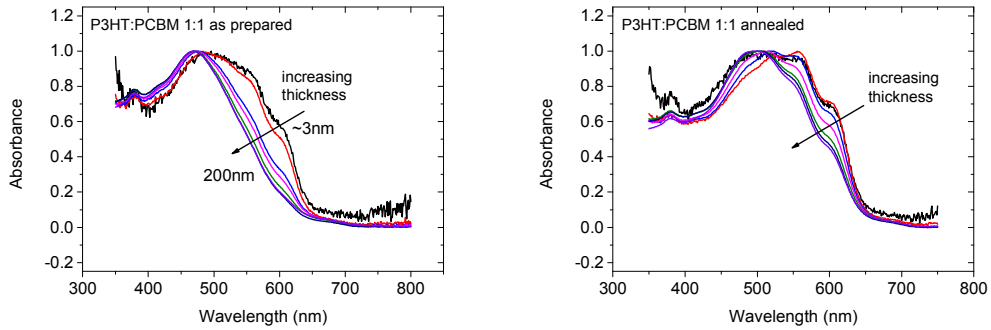

Figure S4: Normalized absorbance spectra of as-prepared and annealed P3HT:PCBM (1:1) measured for different layer thickness.

F) Simulation of Kelvin-data for different DOS distributions:

Work function (WF) data as a function of layer thickness as calculated numerically for various DOS distributions of the LUMO-derived states, including Gaussian, exponential, and combined rectangular-exponential DOS shapes. Also, the electrical potential (ϕ) and the electron density (n) profile is calculated for a 200 nm-thick layer. The numerical procedure is based on solving the Poisson equation with the boundary conditions $\phi(x = 0) = 0$ and $E(x = L) = 0$, where the latter is set by the Kelvin probe experiment, i.e., the electric field is zero at the surface of the layer (see also Pingel et al., *Phys. Rev. B* **2013**, 87, 115209). G_0 was set to 10^{27} $m^{-3}eV^{-1}$ for each case (following Tanase et al., *Phys. Rev. Lett.* **2003**, 91, 216601 and Hulea et al., *Phys. Rev. Lett.* **2004**, 93, 166601). The specific location of the DOS was chosen to provide a reasonable match to the substrate Fermi-level at -3 eV.

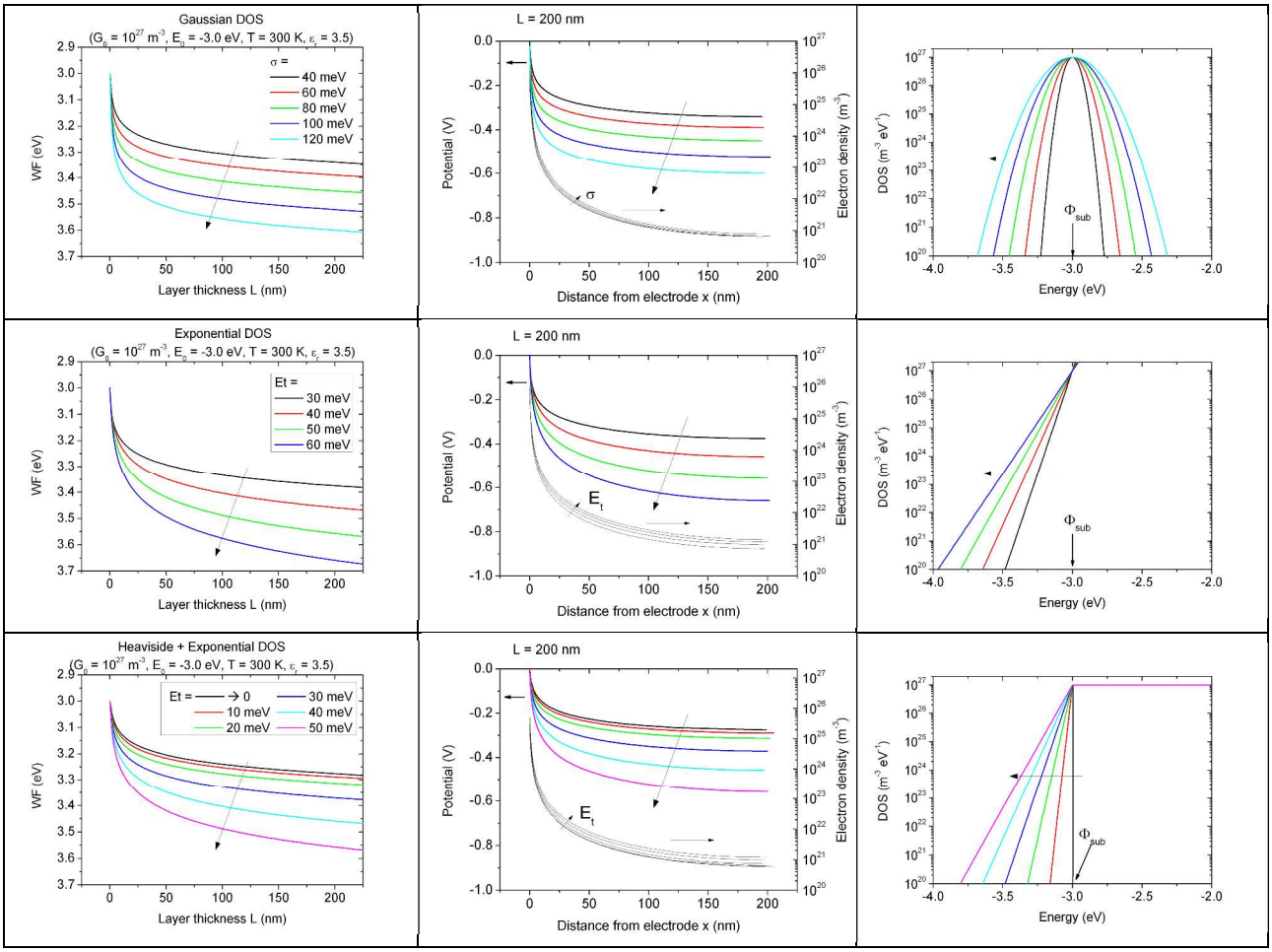

Figure S5: Results from the numerical calculation of Kelvin-data. Left column: WF as a function of layer thickness for different disorder parameters; Middle Column: Electrical potential (lines in color) and carrier density (lines in black) for a layer thickness of 200 nm for different disorder parameters; Right column: corresponding density of state distributions.